JOURNAL OF MATERIALS SCIENCE 31 (1996) 192–198

Soft X-ray image storage in poly(methylmethacrylate)

D. M. SHINOZAKI
Department of Materials Engineering, The University of Western Ontario, London, Ontario, Canada N6A 5B9
P. C. CHENG
Department of Electrical and Computer Engineering, State University of New York, Buffalo, NY 14260, USA

Images stored in resist for soft X-ray lithography or microradiography were found to show a background noise which limits the resolution. This is due to the statistically variable spatial distribution of the photons incident on the resist surface. An estimate of the fundamental noise-limited resolution has been made from the experimental measurement of photon flux incident on the surface and the accurate development rate curves. Monochromatic radiation from a synchrotron source was used.

1. Introduction

Soft X-ray lithography is an imaging method which has been considered for fabricating extremely high-density microelectronic circuits [1]. It is used to replicate fine patterns as one step in the process for making integrated circuits (Fig. 1a). Compared to existing optical methods, the use of soft X-rays promises a much greater depth of field, and much higher resolution. Other competing methods to replicate microstructures have similar limits. Electron-beam writing can be used to generate extremely high-resolution patterns (for example, using contamination writing), but it is a serial method, and is relatively slow in terms of rate of information transfer to the recording medium.

In addition to lithography, the resolution of the polymer film is an important factor in soft X-ray contact imaging, or contact microradiography. Microradiography with hard X-rays is an old method to examine the microstructure of materials, both biological and synthetic (Fig. 1b). However, its resolution can be optimized in the soft X-ray range, ($1 \leqslant \lambda \leqslant 100$ nm) [2], and synchrotron radiation sources dedicated to the generation of extremely high intensities of soft X-rays have become available. One of the principal improvements in the method recently is the widespread use of polymer films to record the images [3].

It is worth noting that the lithographic process has somewhat different requirements than does X-ray contact microradiography. The image for lithography is one of maximum contrast, while the image for microstructural examination is one with a large dynamic range, and a smoothly varying grey scale. The microcircuit fabrication process requires, in addition, a polymer resist which can withstand a variety of severe processing steps, while the contact microradiography process involves developing the image in the near surface region ($\leqslant 25$ nm) to obtain the highest resolution [4].

In both lithography and in contact imaging, the resolution of the image-storage medium has thus been increased by eliminating the limiting grain size of the photographic emulsion. The experimental evidence suggests that the minimum dimension which can be replicated in a soft X-ray lithographic image in poly(methylmethacrylate) (PMMA) is ~ 15 nm [5], which is similar to the limit of resolution suggested for electron-beam writing [6]. This similarity for electrons and X-rays is not surprising because the radiation damage process from X-rays involves the generation of photoelectrons with kinetic energies more than large enough to break polymer bonds ($20 \leqslant E \leqslant 5000$ eV).

The photons are randomly incident on the surface of the resist, and if pixel elements at or near the limit of resolution are considered, neighbouring pixels will absorb statistically different amounts of energy. Smith has outlined a theoretical model to take into account this inhomogeneous distribution of photons in his study of linewidth control in lithography [7]. The present work gives experimental evidence for the effect of this inhomogeneity on the images stored in PMMA resist.

2. Experimental procedure

PMMA with a weight average molecular weight of approximately 450 000 a.m.u. was dissolved in chlorobenzene. This has been used as a standard soft X-ray resist for both lithography and for microradiography. The solutions were spun on to circular glass cover slips using a resist spinner, and subsequently baked to produce thicknesses of approximately 2 μm. The soft

0022–2461 © *1996 Chapman & Hall*

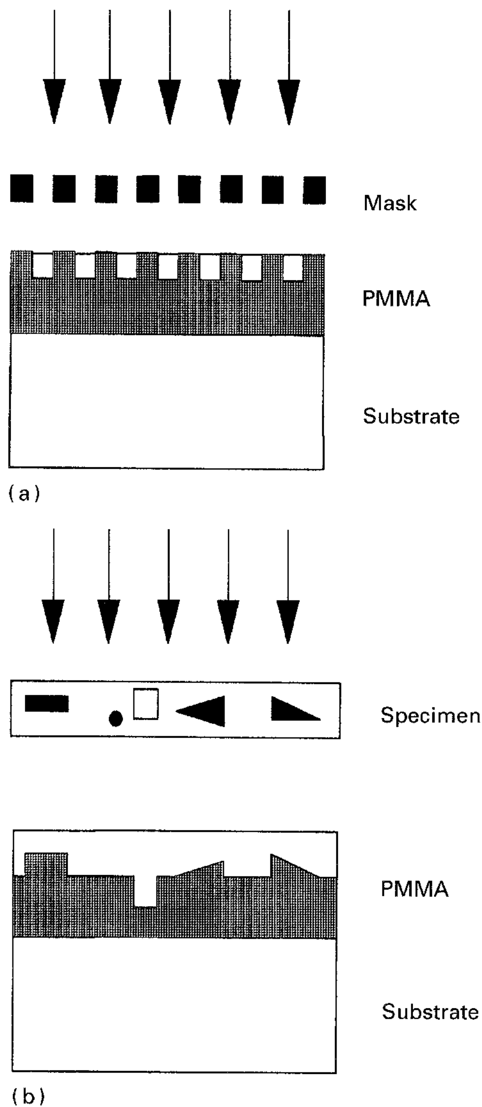

Figure 1 (a) High contrast topographic image in soft X-ray lithography. (b) Continuous tone image in microradiography.

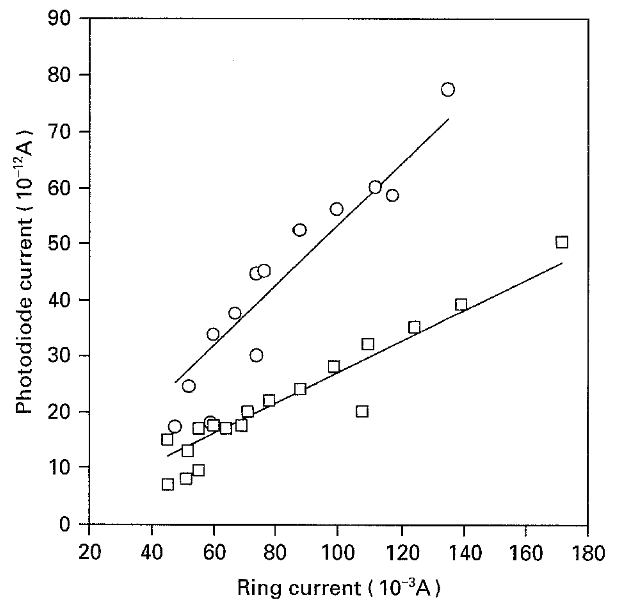

Figure 2 Gold detector photoelectron current versus electron current stored in the synchrotron ring: (□) $\lambda = 3.5$ nm, (○) $\lambda = 1.8$ nm). The monochromator output varies with λ.

X-ray exposures were made using monochromatic radiation from a synchrotron storage ring (Aladdin, University of Wisconsin). The "Grasshopper" monochromator beamline of the Canadian Synchrotron Radiation Facility was used at wavelengths of 1.8 and 3.5 nm. The PMMA film, with the glass substrate backing, was exposed to the beam in a cryo-pumped ultra-high vacuum chamber at pressures of approximately 1×10^{-9} torr (1 torr = 133.322 Pa) or better.

The beam from the monochromator was several millimetres wide and about 2 mm high at the specimen, and it had a non-uniform intensity in cross-section, with highest intensity near the central 1 mm or less. The two-dimensional intensity field was measured using a 20 μm diameter circular aperture step scanned across the beam. A gold "diode" was used as the detector. The PMMA exposures were then restricted to the central area of the beam where the intensity was uniform by using a 200 μm diameter aperture.

The gold "diode" consisted of a gold surface and a Faraday cup surrounding the surface. The incident soft X-ray photons generated photoelectrons which were collected in the Faraday cup. The photoelectron current was measured and the number of photons calculated using the known quantum efficiency of gold [8, 9]. Because the X-ray beam had a uniform intensity over the 200 μm diameter area, the incident photons were uniformly distributed over the entire area.

The uniformity of photon flux over the exposed area then allowed accurate development rate versus dose measurements, and ensured that the statistical roughness observed could be correlated with accurate photon doses.

The dose incident on the specimen was controlled by monitoring the current in the synchrotron storage ring. The radiated output from the ring for a given spectral region was proportional to the stored current. The relationship between the intensity incident on the specimen and the ring current was measured (Fig. 2), and was found to be reproducible over the entire experimental run. The stored electron current decayed with time so the integrated current–time (mA–min) was used as the parameter to measure the incident dose.

The development rates for the resist were measured as developed depth versus time of development in a solution of equal parts (1:1) of methylisobutylketone and isopropyl alcohol. It was known that there was an incubation time at the start of each dissolution process before steady-state dissolution rates were achieved [10]. For each dose, at least five exposures of the same dose were therefore developed for different times and the depths measured using a Tencor profilometer.

2.1. Methods to examine small structures in resist images

Surfaces of resist which are exposed to soft X-rays and subsequently developed are usually examined by scanning electron microscopy (SEM). However, the

radiation sensitivity of the resist is such that such surfaces will ablate in the vacuum under electron bombardment. The doses which effectively evaporate the surface layers of molecules are similar to those used in ordinary SEM. For image formation in the SEM, the incident electron must interact with the molecules of the resist and if the incident electron energy is greater than the bond energy, of the order of a few electron volts, there is a finite probability that the intramolecular bond will break. The probability depends on the absorption cross-section, which is very large for low energies. The energy which does not result in electrons or photons being emitted from the surface is converted to heat or to molecular bond scission and cross-linking. PMMA undergoes chain scission on electron irradiation and eventually evaporates in vacuum at low molecular fragment weight [11, 12].

The effect on the image on the resist surface was illustrated elsewhere [13]. For visibility of surface topographic images in PMMA, the observed resolution at mass losses less than 1% was no better than 100 nm. Thus, for practical purposes, scanning or transmission electron microscopy performed in the standard way to resolve PMMA structures as small as 20 nm or less results in significant mass loss in the first few seconds of examination. The mass loss occurs from the surface and seriously distorts or destroys topographic information. This radiation sensitivity is similar for a wide variety of important commercial polymers.

It should also be noted that radiation damage mechanisms in PMMA do not change for electron energies as low as those used in low-energy SEMs (of the order of hundreds of electron volts). This can be concluded by recent work published on radiation damage kinetics in PMMA resulting from photoelectrons generated by soft X-ray irradiation [12].

SEM examination of topographic variations in PMMA surfaces is therefore not a reliable method for measuring fine-scale surface roughening. Other methods, such as atomic force microscopy, may be applied to record surface topography, but the stress at the contact point greatly exceeds the failure stress of the PMMA and the extent or nature of the deformation-induced distortion of the image has not been clearly measured..

The method used in the present work involves the fabrication of a two-stage replica of the surface. The PMMA coated with about 20 nm AuPd deposited at a shallow angle to the surface, and then subsequently uniformly coated with about 50 nm carbon; both layers deposited by vacuum evaporation. The PMMA is dissolved away and the shadowed replica deposited on a TEM grid. The replicas were examined in a Jeol TEM (100 CX) at an acceleration voltage of 80 kV. Local shadowing angles were measured using calibrated polystyrene spheres of the appropriate size.

To confirm that the soft X-ray exposure and development resulted in a surface roughness, the following replicas were compared: (1) the original PMMA surface, directly after spinning and baking; (2) after exposure to soft X-ray irradiation and no development; (3) after exposure and development. Each specimen was irradiated with soft X-rays through a TEM copper grid, so the boundary between exposed and unexposed regions would be revealed.

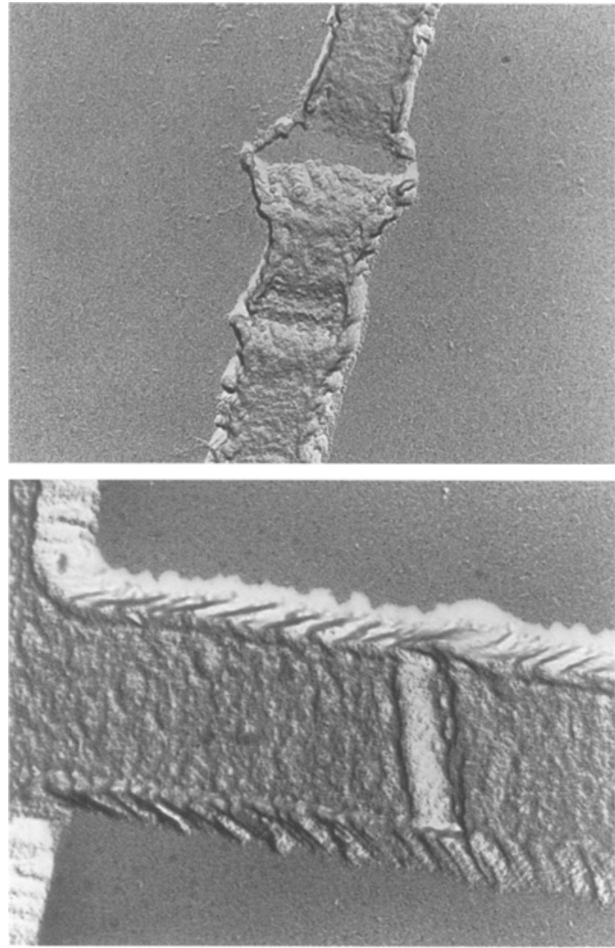

Figure 3 Transmission electron micrograph of a replica of a soft X-ray image stored in PMMA. The specimen is an AlCu conducting line. The line is 1 μm wide and is on a substrate of 120 nm silicon nitride. Internal fine-scale microstructure of the alloy is visible down to scales at which background noise becomes significant.

The effect on microradiographic images is shown in Fig. 3. The background noise in the surface of the exposed and developed resist is clearly visible. For lithographic imaging, as pointed out by Spiller and Feder [1], the dose at the resist should be large, and the contrast in the developed resist image should be maximized. In regions of the resist which absorb large doses (transparent regions of the mask) the resist is completely dissolved away, and the background noise is not observed. In the optimum lithographic process, the opaque regions of the mask suffer no irradiation and remain smooth. However, in the region near the mask boundary, the absorbed X-ray dose varies with position, increasing smoothly to the high dose region. This is the critical region of the lithographic image which defines the sharpness of the edge. The background noise has an influence on the quality of this edge. For many applications requiring only micrometre scale resolution, the background noise is not a significant problem and may be ignored.

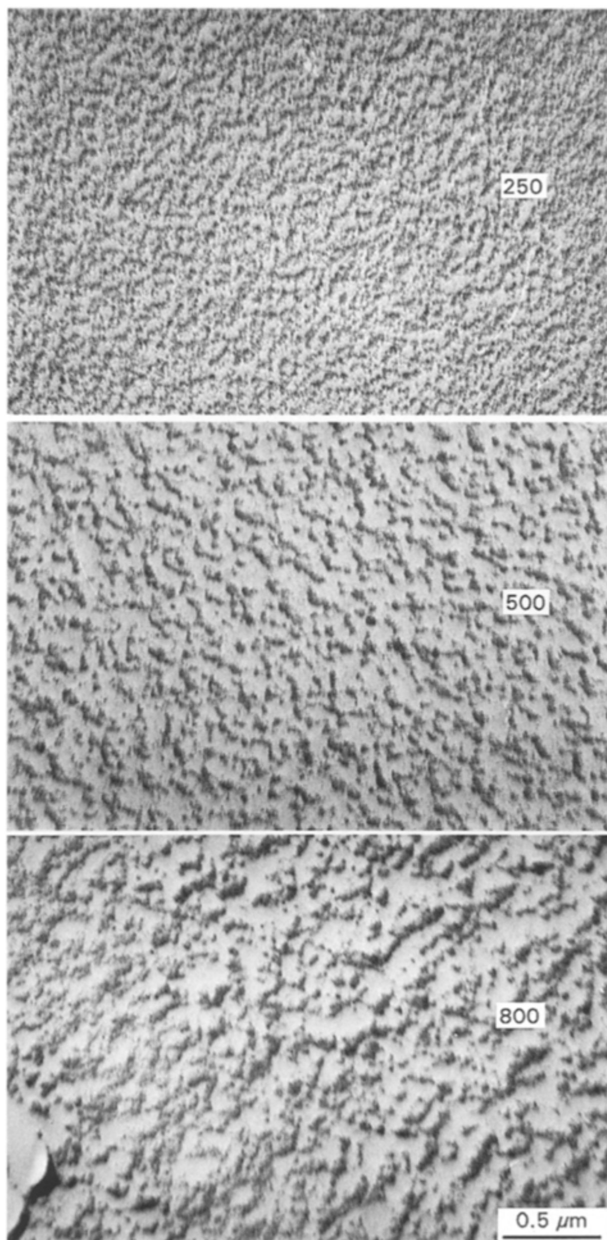

Figure 4 TEM replica of PMMA surface which has been exposed to 1.8 nm soft X-rays and developed in 1:1 MIBK:IPA for only 5 s. The doses are given in terms of mA min^{-1}.

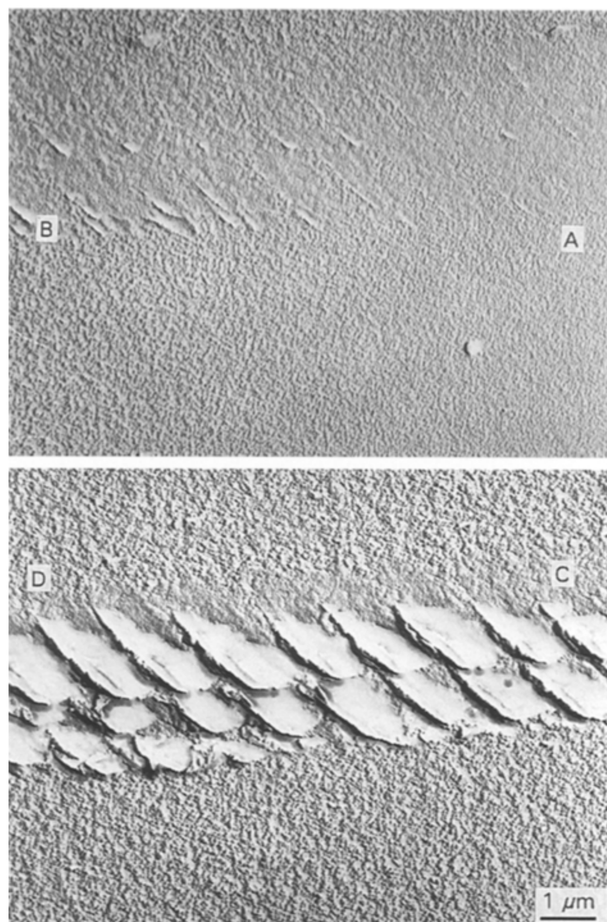

Figure 5 TEM replica of a profilometer trace in PMMA. The one trace starts in unirradiated material at A and moves to the irradiated zone in the lower micrograph at D. The exposure in the zone CD is $800\ \text{mA min}^{-1}$ with 1.8 nm radiation, and the development is similar to that in Fig. 4.

3. Results and discussion

The noise in the resist surface is shown in Fig. 4 as a function of increasing dose. The doses shown (250, 500 and $800\ \text{mA min}^{-1}$) are typical for microradiographic images. The noise increases from the $250\ \text{mA min}^{-1}$ low dose image to the $800\ \text{mA min}^{-1}$ medium dose. These images are for development in 1:1 MIBK:IPA for 5 s only, which is a very light development for microradiographic purposes.

The noise inherent in the replica technique is seen in Fig. 5, in which the two images are from one specimen, the top one from the unirradiated region and the bottom image from the $800\ \text{mA min}^{-1}$ exposure. Both regions have been developed in the same way as the specimens in Fig. 4. The profilometer track is observed to start at A and progress to B, at which the profilometer deformation track is visible. The profilometer track (CD) is much clearer in the irradiated region in the bottom figure. It is obvious that the profilometer deforms the irradiated region much more than the unirradiated region, and subsequent depth measurements are somewhat in error. The correction is, however, relatively small. It is interesting to note that the low molecular weight PMMA has a much lower yield stress.

The doses shown here are modest exposures, and in recording high-resolution microradiographic images, doses as high as $1000\ \text{mA min}^{-1}$ are common. The absorbed energy for the two wavelengths are shown as a function of depth in the resist in Fig. 6a and b for exposures tested in the present experiments. It should be noted that the numbers of photons incident on the resist vary with wavelength, because the ring output and monochromator efficiency vary. These plots are calculated from measured photon outputs at the specimen using the gold "diode" calibrations.

The measured development rates are shown in Fig. 7. The data are consistent with earlier work which suggests that $G(s)$, the number of chain scissions per 100 eV absorbed, for PMMA at 2 nm is 1.28 and there is no dependence on wavelength in the soft X-ray range [12]. There is a slight non-linearity which appears in Fig. 7 as a larger slope at high doses. This may be related to the shape of the dissolution rate versus molecular weight curve seen in Greeneich's work [14]. His original data are replotted on linear scales

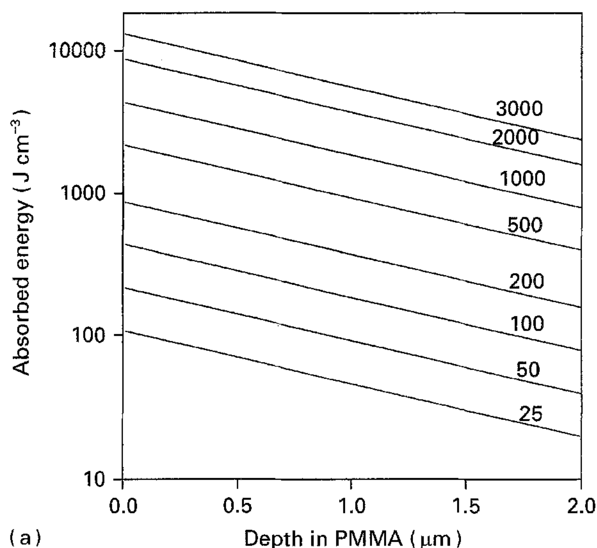

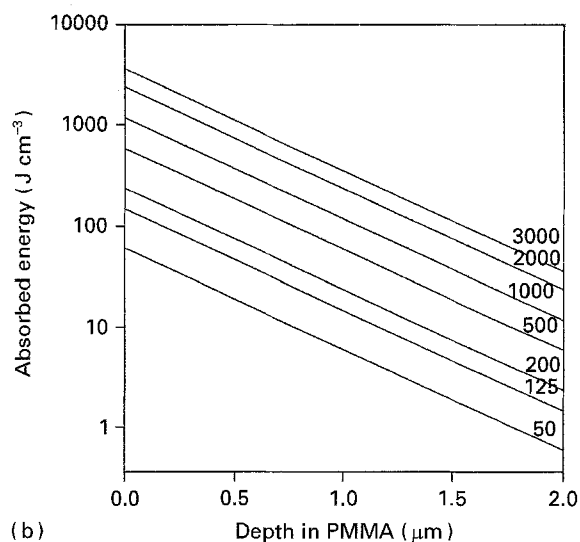

Figure 6 Calculated absorbed energies as a function of depth in the resist for (a) 1.8 nm radiation, and (b) 3.5 nm radiation. The incident doses are measured in mA $\min^{-1}$ (3000, 2000, etc.).

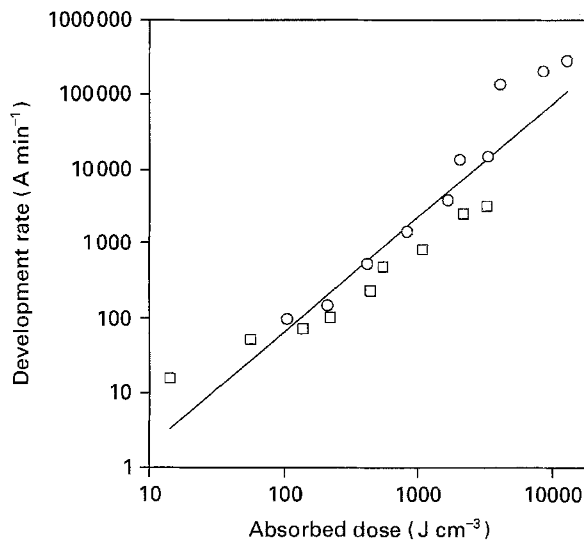

Figure 7 Development rate for PMMA exposed to (○) 1.8 nm and (□) 3.5 nm radiation.

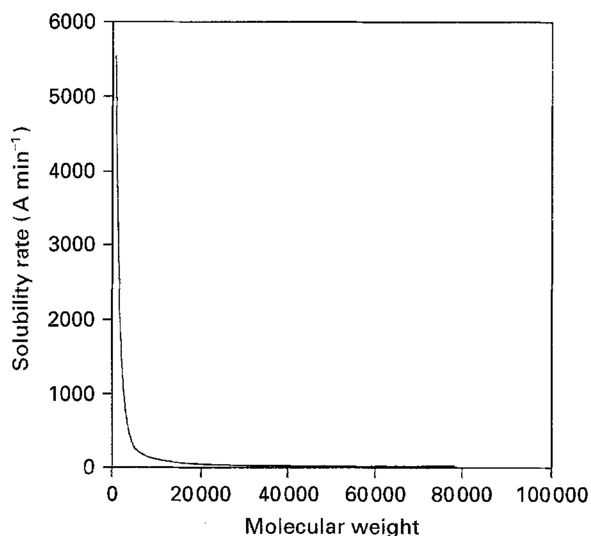

Figure 8 Solubility rate for PMMA developed in 1 : 1 MIBK : IPA versus molecular weight (replotted on linear scales from [14]).

in Fig. 8. There is a very sharp cut-off in dissolution rate for PMMA at molecular weights under 10 000. The molecular weight distribution for the unirradiated and for heavily irradiated PMMA are given elsewhere [12], which shows that even at doses of 3000 mA $\min^{-1}$ or higher, only a small fraction of the polymer has degraded to molecular weights below 10 000. The dissolution process involves molecules with a broad range of molecular weights. The measured dissolution rates might then be expected to increase rapidly in the high dose range where the low molecular weight tail to the distribution changes rapidly with dose.

3.1. Calculated background noise

Knowing the average dose incident over the entire exposed area, an average photon dose can be calculated as in Table I. These are numbers for a 2 nm square pixel. The requisite number of photons can be deposited into pixel "bins" and the peak to valley distribution plotted as in Fig. 9. The width of the band is a measure of the statistical noise in terms of the numbers of photons incident on the pixels.

TABLE I

Measured dose (mA $\min^{-1}$)	Number of photons/ 2 nm × 2 nm pixel
3000	112.4
800	30
200	7.48
125	4.68

The experimentally measured development curve can be fitted to the function

$$R = 0.0107\,D^{1.813} \qquad (1)$$

where R is the rate of development (A $\min^{-1}$) and D is the absorbed dose (J cm^{-3}).

In a uniform exposure, the resist is irradiated with some average exposure measured from the gold

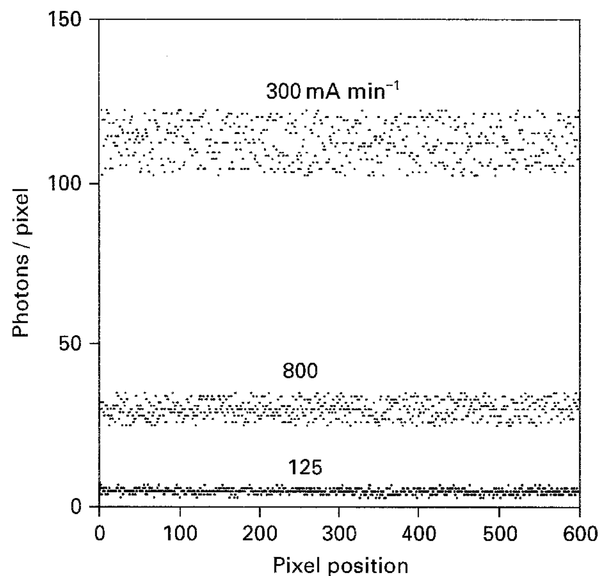

Figure 9 Numbers of photons incident on pixels (2 nm × 2 nm) for typical microradiographic exposures.

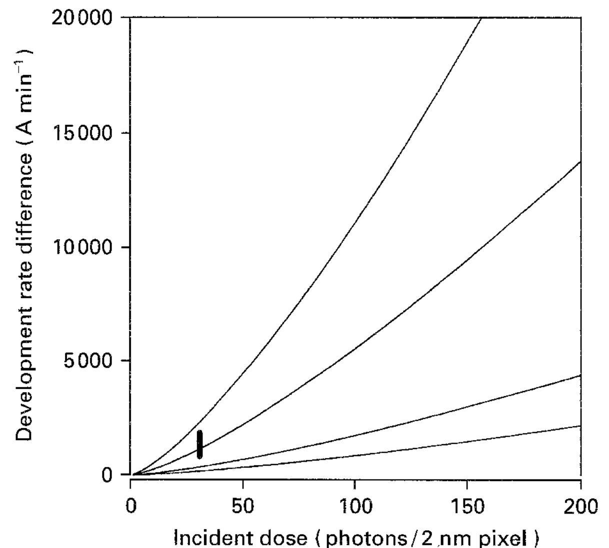

Figure 10 Maximum development rate difference for different exposures. The vertical heavy black bar is that measured for an 800 mA min^{-1} exposure. The k factor is 0.25, 1, 10 and 40 from top to bottom.

detector as the number of photons of the given wave length per unit area per unit time. But individual pixels within the sample area are exposed to values which vary statistically around this mean. The exposure is given as n_0 photons incident on the area of the pixel, and for a photon exposure in which each absorption event is independent of every other, one standard deviation of exposure is $n_0^{1/2}$ [1].

The absorbed dose can be replaced by a function of the number of photons, n_0, of energy, $E_{h\nu}$, incident on an area, A_0, and the absorption coefficient, μ

$$R = 0.0107\left(\frac{\mu n_0 E_{h\nu}}{A_0} e^{-\mu z}\right)^{1.813} \quad (2)$$

Substituting appropriate values for $E_{h\nu}$, z and μ for the experiment, the rate of development can be estimated at a given wavelength as a function of n_0, the number of photons incident on the pixel of the given area, A_0 (in these estimates, a 2 nm × 2 nm pixel is used). Accurate experimental absorption coefficients for the soft X-ray range have been published recently [15]. For a random distribution of photons over the area of the exposed resist, a pixel will be exposed to $n_0 \pm n_0^{1/2}$ photons. The maximum peak to valley developed height difference can be estimated by calculating the maximum difference in rates of development for the two extreme doses. The maximum development rate difference can be calculated for different pixel areas kA_0, for which the dose is $kn_0 \pm kn_0^{1/2}$

$$\Delta R = 13.2\frac{n_0^{1.31}}{k^{1/2}} \quad (3)$$

The maximum development rate range ΔR decreases as the pixel size increases because the maximum photon dose range increases as a function of $k^{1/2}$, and the area of the pixel increases as a function of k. Thus, for a given average exposure, the surface becomes smoother for larger pixel size. The development rate difference so calculated is plotted as a function of the number of photons incident on the pixel for different pixel dimensions, k, in Fig. 10.

Using the development rate difference, and knowing the development time, the measured peak to valley height range is shown for a typical 800 mA min^{-1} exposure as a heavy vertical bar superimposed on the calculated curves. Althogh the error bar is large, it is possible to estimate the pixel size to be in the range 2–5 nm. This is smaller than the smallest structures observed in PMMA, but corresponds to the suggested theoretical limit of 5 nm. For practical microradiographic imaging, useful resolution might be typically two to three times larger than this limit.

It should be noted that this estimate does not include lateral development of the resist. Small protuberances in the dissolving resist surface will develop rapidly in directions parallel to the resist surface. Development rates are so large for typical exposures in PMMA that 1–5 nm structures will be dissolved very rapidly. Noise-limited images can only be observed for very lightly developed surfaces. Techniques such as direct electron microscopy of the polymer surface cannot be used to examine such small structures.

4. Conclusion

The noise in the resist image due to the statistical distribution of photons incident on the polymer surface has been observed. The topographic roughness due to the pixel to pixel development rate differences has been quantitatively measured and shown to correlate with the expected statistically inhomogeneous distribution of photons. An estimate of the fundamental resolution limit of the PMMA resist has been made by comparing the measured roughness with that expected for different pixel dimensions. This is similar, within experimental error, to that predicted from photoelectron path length dimensions in the resist. These dimensions are significantly smaller than those which have been experimentally observed in the litera-

ture. This discrepancy may be due to the inherent difficulty in examining small structures in radiation-sensitive polymers.

References

1. E. SPILLER and R. FEDER, in "Topics in Applied Physics", Vol. 22, "X-ray Optics and Applications to Solids", edited by H. J. Quiesser (Springer, Berlin, 1977) p. 35.
2. D. SAYRE, J. KIRZ, R. FEDER, D. M. KIM, E. SPILLER, *Ann. N.Y. Acad. Sci.* **306** (1978) 286.
3. D. M. SHINOZAKI and R. FEDER, in "Treatise in Materials Science and Technology", Vol. 27, "Analytical Techniques for Thin Films", edited by K. N. Tu and R. Rosenberg (Academic Press, New York, 1988) p. 111.
4. J. KIRZ and D. SAYRE, in "Synchrotron Radiation Research", edited by H. Winick and S. Doniach (Plenum Press, New York, 1980) p. 277.
5. D. C. FLANDERS, *Appl. Phys. Lett.* **36**(1) (1980) 93.
6. S. MACKIE and S. P. BEAUMONT, *Solid State Technol.* August (1985) 117.
7. H. I. SMITH, *J. Vac. Sci. Technol.* **B4**(1) (1986) 148.
8. R. B. CAIRNS and J. A. R. SAMSON, *J. Opt. Soc. Am.* **56** (1966) 1568.
9. B. L. HENKE, J. P. KNAUER and C. PREMARATNE, *J. Appl. Phys.* **52** (1981) 1509.
10. R. FEDER, private communication.
11. H. HIRAOKA, *IBM J. Res. Develop.* (1977) 121.
12. B. W. YATES, D. M. SHINOZAKI, *J. Polym. Sci. B. Polym. Phys.* **31** (1993) 1779.
13. D. M. SHINOZAKI and B. W. ROBERTSON, in "X-ray Microscopy", edited by P. C. Cheng and G. J. Jan (Springer, Berlin, 1987) p. 105.
14. J. S. GREENEICH, *J. Electrochem. Soc. Solid State Sci. Technol.* **122** (1975) 970.
15. B. W. YATES, D. M. SHINOZAKI, A. KUMAR and W. J. MEATH, *J. Polym. Sci. B Polym. Phys.* **30** (1992) 185.

Received 13 June 1994
and accepted 22 June 1995